Journal of Fluids and Structures (2001) **15,** 427–443
doi:10.1006/jfls.2000.0346, available online at http://www.idealibrary.com on IDEAL®

QUANTITATIVE IMAGING OF THE WAKE OF A CYLINDER IN A STEADY CURRENT AND FREE-SURFACE WAVES

D. Rockwell, J.-C. Lin, O. Cetiner, K. Downes and Y. Yang

Department of Mechanical Engineering and Mechanics, 354 Packard Laboratory 19 Memorial Drive West, Lehigh University, Bethlehem, PA 18015, U.S.A.

(Received 4 September 2000, and in final form 6 November 2000)

The technique of high-image-density particle image velocimetry (PIV) can lead to instantaneous, global representations of the wake of a cylinder in a steady current and free-surface waves. Approaches to characterizing the complex patterns of the wake are described for several classes of experimental systems. Emphasis is on imaging in different planes, with the aim of providing insight into the quasi-two- and three-dimensional features of the near-wake.

1. INTRODUCTION

During the past decade, application of particle image velocimetry to the wakes of cylinders has yielded quantitative insight in a wide variety of investigations. They are described in works edited by Eckelmann *et al.* (1992) and Bearman & Williamson (1998), and the conference abstracts provided by Bearman *et al.* (2000). Further overviews are given by Rockwell (1998, 2000).

High-image-density particle image velocimetry, based on film as a recording medium, was employed in the investigations summarized by Rockwell *et al.* (1993). Representative images therein illustrate both the quasi-two- and three-dimensional features of the near-wakes of cylinders. More recent studies that employed film-based systems have focused on the issues of: Reynolds number sensitivity of the near-wake vortex patterns (Lin *et al.* 1995); simultaneous existence of small- and large-scale concentrations of vorticity in the near-wake (Chyu & Rockwell 1996*a*; Sheridan *et al.* 1997); timing of initially-shed concentrations of vorticity in relation to oscillations of the cylinder (Gu *et al.* 1994; Sheridan *et al.* 1998); three-dimensional structure of the near-wake of a stationary cylinder (Lin *et al.* 1996*b*; Chyu & Rockwell 1996*b*; Brede *et al.* 1996) and an oscillating cylinder (Towfighi & Rockwell 1994; Gu & Rockwell 1995); control of the near-wake by three-dimensional fluid injection (Lin *et al.* 1995) and interaction between stationary and deformed free-surfaces with the near-wakes of stationary and oscillating cylinders (Lin *et al.* 1996*a*; Sheridan *et al.* 1997). The consequence of spatial resolution of the image acquisition system on interpretation of small- and large-scale vortex interactions in the near-wake region is assessed by Lin & Rockwell (1997).

Recent investigations that employ the digital version of particle image velocimetry (DPIV) have provided substantial insight into the near-wake structure of a cylinder. The three-dimensional features of the wake from a stationary cylinder were addressed by Wu *et al.* (1994, 1996). More recently, the emphasis of most investigations has been on

0889–9746/01/040427 + 17 $35.00/0

quasi-two-dimensional patterns of the near-wake structure of a stationary and an oscillating cylinder. This series of investigations includes: the wake system from arrangements of cylinders (Sumner *et al.* 1998, 2000); the wake from an accelerating cylinder (Noca *et al.* 1998, 1999); wakes from oscillating cylinders (Techet & Triantafyllou 1998; Atsavapranee *et al.* 1998); the wake structure from a cylinder in orbital motion (Williamson *et al.* 1998); and the two- and three-dimensional wake from a stationary cylinder in presence of a free-surface (Lang & Gharib 1998).

In nearly all of the foregoing investigations, presentations of patterns of instantaneous velocity and vorticity, as well as phase- or time-averaged representations of them, has been a primary goal. Of course, once quantitative images are attained, a range of possibilities for interpretation become available, as described by Rockwell (2000). For example, employment of topological concepts based on critical point theory, a snapshot version of proper orthogonal decomposition (POD), as well as a variety of other approaches can be invoked. Furthermore, direct links to a range of theoretical, vorticity-based models can be attained. These models represent concepts of: convective instabilities of the near-wake; forces on the cylinder in relation to patterns of velocity and vorticity; generation of acoustic power in coupled wake–resonator systems; and the onset of critical states in swirling flows.

Of all of these conceptual frameworks for interpreting PIV images, the most relevant to our present considerations is the relationship between the forces on the cylinder and the space–time imaging of the cylinder wake, for either a stationary or an oscillating cylinder. For the situation where the vorticity is confined to the field of view during the process of vortex shedding, Lin & Rockwell (1996) and Zhu *et al.* (2000) have employed the vorticity moment concept described, for example, by Lighthill (1986) to determine either the unsteady forces or the time integral of the unsteady forces acting on a cylinder. In fact, the theoretical concept advocated by Wu (1981) and Lighthill (1986) has been further developed by Noca (1996) and Noca *et al.* (1997), with the aim of accounting for all of the previously generated vorticity that is not contained within the field of view of the PIV imaging system. In essence, this involves a control volume approach. Unal *et al.* (1997) developed a control volume technique based on momentum concepts and, in a parallel and complementary investigation, Noca (1997) and Noca *et al.* (1999) arrive at a different, but presumably, equivalent momentum-based control volume expression. More recently, Noca *et al.* (1999) provide a critical assessment of various control volume representations and, in addition, formulate a type of flux equation that requires knowledge of only the parameters along the boundary of the control surface. Application of particle image velocimetry (PIV) to the assessment of forces on a cylinder clearly involves a number of limitations, as described in the foregoing citations. Irrespective of the degree of approximation, however, links to theoretical concepts have clearly been established, thereby allowing more meaningful interpretation of quantitative images.

The wake from a cylinder can take on a variety of forms, depending upon the nature of the incident current (steady flow), the wave motion, or a combination of them. By now it is well known that even for the comparatively simple system of a stationary cylinder in a current, the near-wake exhibits a range of possible states. When a stationary, vertical cylinder is immersed in a wave, one expects particularly complex states of the wake, due to the elliptical particle trajectories of the wave motion and their variation along the span of the cylinder. Furthermore, elastic or controlled oscillation of the cylinder can further modify the nature of the wake. Interpretation of these representative wake patterns in relation to the loading on the cylinder can be guided by the conceptual frameworks outlined by Wu (1981) and Lighthill (1986). Central to this interpretation, of course, is a quantitative knowledge of the wake structure, preferably in terms of vorticity.

The present aim is to describe selected imaging configurations and representative images that address complex features of the near-wakes of cylinders. An overview of experimental approaches and generic features of imaging systems is followed by descriptions of arrangements that allow simultaneous orthogonal views and dual views of the near-wake.

2. OVERVIEW OF EXPERIMENTAL APPROACHES

All of the investigations herein employ one of a variety of continuous wave Argon-ion lasers as an illumination source, either a rotating, multi-faceted polygon mirror or an oscillating flat mirror to induce rapid scanning of the laser beam, and one of several types of 35 mm film (motor-driven) cameras for image acquisition.

An Argon-ion laser, with a maximum power rating between 5 and 25 W, generated a continuous beam of approximately 1 mm diameter. This beam then impinged upon either the rotating or oscillating mirror, which scanned the laser across the region of interest. For both types of mirror systems, the aim was to provide relatively high-intensity illumination from a continuous laser source. The effective pulse rate of the illumination was dictated by the laser-scanning rate. A major advantage of laser scanning is that the total power of the laser beam illuminates each particle as it sweeps across the flow. Moreover, generation of multiple-pulsed images of particles is easily achieved by adjusting the scanning rate relative to the shutter speed of the camera. A further virtue of this scanning illumination technique is that qualitative patterns of particles can be continuously observed in the plane of the laser sheet immediately prior to and during acquisition of PIV images. This approach allows effective monitoring of the overall features of the flow. A disadvantage of the laser scanning approach is an effective reduction in illumination time of each particle at higher scanning frequency, which is required at higher values of flow velocity. In addition, the retrace time of the oscillating mirror, whereby the beam traces back to its initial position during each scanning cycle, or splitting of the beam at the edge of a polygon (multi-faceted) rotating mirror, can result in a reduction of the effective duty cycle of the scanning laser beam if the system is not properly designed (Rockwell *et al.* 1993). For the investigations described herein, the rotating polygon mirror had either 8, 48 or 72 facets. It was controlled externally by an analog system in order to maintain the revolution rate to within an accuracy of 0.1%. In effect, the typical scanning rate of the laser beam across the plane of interest using the polygon mirror ranged from approximately 100 to 700 cycles/s. Alternately, an oscillating mirror was employed. It was mounted on a galvanometer scanner, which was externally controlled by a driver unit. This arrangement is effective for lower scanning rates, extending up to approximately 100 Hz; such scanning rates are required at lower values of velocity. Over this range of operation, the oscillating mirror system is preferred to the rotating polygon mirror, which yields significant uncertainty of the laser-scanning rate at low values of mirror rotation rate. For the experimental configurations described herein, the oscillating mirror is preferred over the rotating mirror for certain end views, i.e., crossflow planes.

For all of the present experiments, the flow was seeded with metallic coated, hollow plastic spheres having a nominal diameter of 12–14 μm. The required number of particles can be estimated *a priori*. The relevant image density parameter, originally defined by Adrian & Yao (1984), is $N_I = C\Delta z_o A_I/M$, in which C is the mean number of particles per unit volume, and Δz is the thickness of the laser sheet. The interrogation cell employed for evaluation of the velocity vector has an area of A_I/M on the plane of the laser sheet. If $N_I \gg 1$, there is a high probability of finding many particle images in the interrogation cell. For the present experiments, the representative interrogation area was 0.5 mm^2, the thickness of the laser sheet was approximately 1 mm, and values of magnification ranged from

1:6 to 1:11. The interrogation volume contained approximately 30–60 particle images, which substantially exceeds the high image density criterion.

Multiple-pulsed illumination was attained by maintaining the camera shutter open during three to five scans of the laser beam across the plane of interest. Keane & Adrian (1990, 1991) undertook theoretical and numerical analyses to assess the performance criteria of multiple- versus double-pulsed systems, as well as other features of PIV approaches employing autocorrelation techniques. As pointed out by Adrian (1991), a four-pulse single exposure that contains N_I particles yields a self-correlation peak of height $4N_I$, a first correlation peak of height $3N_I$ and so on. The overall performance is essentially equivalent to that of a double-pulse image pattern obtained from $3N_I$ particles at the same time spacing Δt.

The multiply- pulsed patterns of particle images were recorded on high-resolution 35 film. It provides an effective pixel size, as calculated from one-half of the line pairs per millimeter, of 5 μm × 5 μm, and an effective format of 7000 × 4800 pixels or, equivalently, a total of $33{\cdot}6 \times 10^6$ pixels. This concept of pixel equivalents for a film-based format relative to the pixel format of video/digital camera systems is assessed by Adrian (1995). It is crucial that the 35 mm negatives are digitized at sufficiently high resolution. For the present experiments, the digitizing process was executed at 125 pixels/mm.

Several types of motor-driven 35 mm cameras were employed to acquire sequential images of the flow. Depending upon the time scale of the flow event, which was relatively slow in the water systems described herein, it was possible to attain adequate temporal resolution to allow reconstruction of cinema sequences. Standard, motor-driven 35 mm cameras had framing rates in the range of approximately 5–10 frames/s. In addition, a specially designed framing camera allowed acquisition of images at a rate of 60 frames/s. This system is the basis of the cinema PIV approach described in detail by Lin & Rockwell (1994, 1999). It provides an effective transfer rate of 2×10^9 equivalent pixels/s.

For all camera systems, an image-shifting mirror was located immediately in front of the lens system. While the camera shutter was open, the mirror was subjected to a prescribed rate of rotation by a galvanometer scanner. This image shifting, in essence, provides a constant bias displacement to all particle images, which is removed following the interrogation procedure to evaluate the velocity field. Such a bias is necessary in order to preclude directional ambiguity in regions of negative or reverse flow. In the present investigations, the typical dimensions of the bias mirror were 50 mm × 30 mm × 1 mm. Full details of the bias mirror concept are described by Adrian (1986). In order to ensure that the motion of the bias mirror does not distort the pattern of particle images, it should be operated within a specific range of parameters. If caution is not exercised, systematic distortions of the patterns of particle images may arise, as described by Oschwald *et al.* (1995), Lee *et al.* (1996) and Raffel & Kompenhans (1995). The latter two groups of investigators propose techniques to correct for systematic errors.

Irrespective of the type of image acquisition system, it is important to consider the paraxial recording criterion. Let $x_{\max}$ represent the maximum in-plane location of a particle measured from the centerline of the camera lens, and d_o the object distance; the ratio $x_{\max}/d_o$ should be minimized (Lourenco & Whiffen 1986; Adrian 1991). This condition ensures that the consequences of out-of-plane motion are small when determining the velocity field from in-plane measurements.

In addition to the foregoing considerations, Keane & Adrian (1990, 1991) show, via theoretical concepts and numerical simulations, that the best overall performance of a double-pulsed imaging system is attained when: (i) the in-plane displacement of a particle is less than one-fourth the width of the measuring volume (cell); (ii) the out-of-plane displacement of a particle is less than one-fourth the thickness of the laser sheet; and (iii) the

velocity variation over the measuring volume is less than 20% of the characteristic velocity within the volume. Criterion (ii) is particularly important for end view measurements, i.e., measurements in the crossflow plane of a highly three-dimensional flow. Design of the imaging systems described herein aimed to satisfy these criteria.

In the following, three different classes of PIV arrangements are considered: (i) an orthogonal view system, which allows simultaneous acquisition of images in orthogonal laser sheets; (ii) a dual view system, which provides simultaneous acquisition of images in two adjacent fields of view in the same plane for cases where the region of interest has a very high aspect ratio; and (iii) a dual view system, which also involves adjacent fields of view, but with the aim to preclude blind areas, or shadow effects, due to use of a long object distance in presence of a stationary or oscillating body.

3. ORTHOGONAL VIEW SYSTEM FOR THREE-DIMENSIONAL FLOWS

The objective of this class of imaging is to acquire space–time representations of the flow in two orthogonal views, i.e., in two planes oriented perpendicular to each other. This approach allows simultaneous characterization of the quasi-two- and three-dimensional structure of the flow. An important physical issue is the degree to which motion of the body attenuates large-scale three dimensionality, and whether the nature of small-scale spanwise three dimensionality is attenuated, or even enhanced, by the body motion. This issue is generic to oscillating bodies undergoing not only transverse motion, but also in-line and orbital motions relative to an incident, steady current. The nature of the three-dimensional structure from a stationary cylinder has been the subject of intense investigation as reviewed by Williamson (1996*b*), who describes numerical, theoretical and experimental investigations. For our present purposes, selected experimental studies are of interest. Remarkable insight has been provided by the visualization studies of Hama (1957), Gerrard (1978) and Williamson (1988, 1992, 1996*a*). Corresponding application of particle image velocimetry to characterize patterns of instantaneous velocity, streamlines and vorticity were initially undertaken along the span of the stationary cylinder, and at a transverse location corresponding to the outer edge of the wake, by Rockwell *et al.* (1993) and Wu *et al.* (1994, 1996). Subsequent studies of Chyu & Rockwell (1996*b*), Lin *et al.* (1996*b*) and Brede *et al.* (1996) used space–time imaging to determine patterns of velocity and vorticity across the entire crossflow plane in the near-wake. To date, the quantitative patterns of streamwise vorticity in the near-wake of a cylinder undergoing transverse oscillations have not been characterized.

A schematic of an orthogonal view system is given in Figure 1. It involves a single laser beam and two rotating polygon (multi-faceted) mirrors, as well as two bias mirror-camera units. Details of this arrangement and its application to a variety of oscillating cylinder systems are given by Cetiner & Rockwell (2000). A major challenge of orthogonal laser sheet PIV is the interference of one laser sheet with imaging in the other sheet. For example, if one attempts to obtain patterns of particle images in the side view, the high intensity of the end view laser sheet intersects the side view sheet. This intersection makes it impossible to attain adequately resolved particle images over a significant region of the field of view. To circumvent this difficulty, it is desired to shut off the illumination of the end view sheet when imaging in the side view, and conversely. This is accomplished by employing a Pockels cell arrangement, as indicated in Figure 1. The Pockels cell rapidly switches the laser beam from its colinear (throughput) mode to its deflected mode. In doing so, the beam is shifted from a position that generates a side view laser sheet, which is eventually transmitted to camera 1, to an end view laser sheet, which is recorded by camera 2.

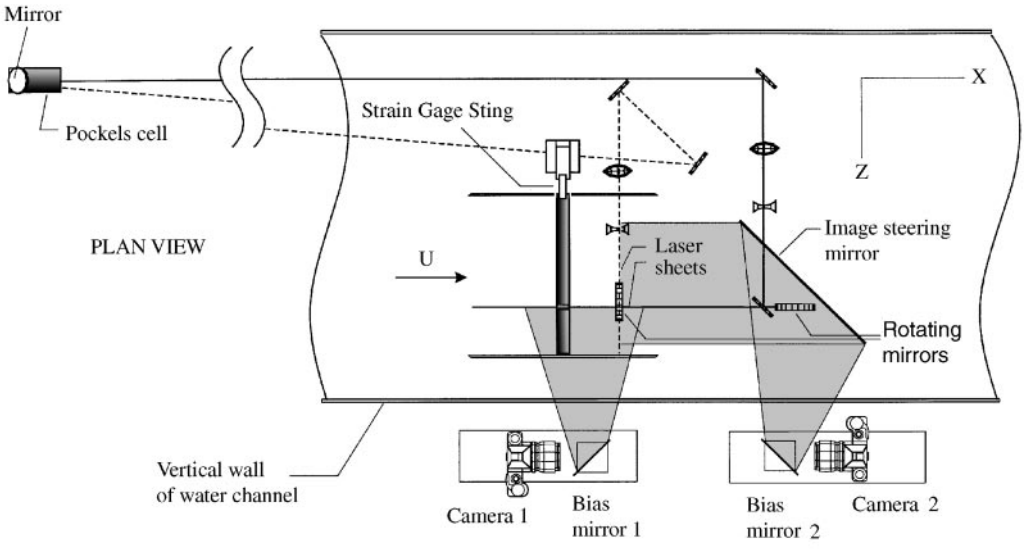

Figure 1. Schematic of arrangement for space–time imaging in two orthogonal views which are defined by two laser sheets. A single laser generates the laser sheets via deflection of the laser beam through a Pockels cell.

More specifically, the end view of the laser sheet was generated as follows. The beam from the Pockels cell was deflected at an angle as represented by the circular mirror arrangement on the side of the Pockels cell. This deflected mode is designated by the dashed line. The beam eventually impinged upon two successive steering mirrors. It was then transmitted through a series of focusing optics and eventually impinged upon the rotating mirror that generated a scanning laser beam over a plane orthogonal to the incident flow U. The field of the end view of the laser sheet is designated by the gray shaded area. The pattern of particle images was transmitted to the bias mirror 2, then reflected to the back of camera 2. An analogous concept was employed for the side view. The entire system comprising the Pockels cell and the camera-bias mirror units 1 and 2 were controlled by a laboratory microcomputer. The time delay between the throughput and deflected laser beam modes of the Pockels cell was approximately 70 ms. This laser switching arrangement thereby provides multiplexing of the side and end view image acquisition. Such multiplexing allows a space–time reconstruction in the two orthogonal views, whereby the image sequence is essentially synchronized, with the aforementioned time delay. The values of magnification of cameras 1 and 2 were 1 : 6 and 1 : 7·8. The fields of view in the side and end views were, respectively, 206 mm × 133 mm and 223 mm × 164 mm. Typically, a total of 6111 and 4720 velocity vectors were obtained for the side and end views, respectively. Representative excerpts from the synchronized sequences of side and end view images of vorticity are exhibited in Figure 2 for the case of a cylinder undergoing transverse oscillations at a value of $A/D = 0{\cdot}96$, in which A is the amplitude of the cylinder motion, and D is the cylinder diameter. The Reynolds number is Re = 1238. It is evident that projections of streamwise vorticity exhibited in the end view sequence can have substantial values of peak vorticity and circulation. In fact, the peak values of these vorticity concentrations are of the order of 13 s^{-1} in comparison with representative concentrations in the side view having 30 s^{-1}. It is therefore apparent that cross-stream oscillations can effectively attenuate larger modes of

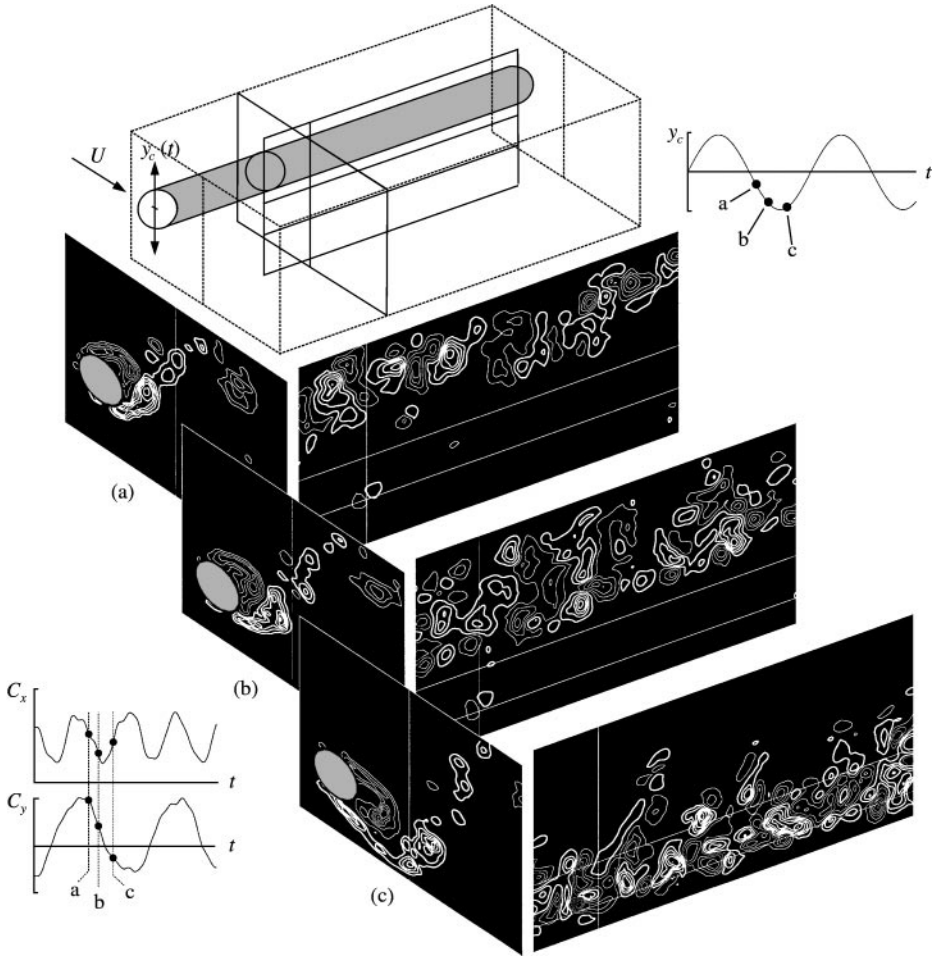

Figure 2. Space–time imaging in orthogonal views of vortex formation from an oscillating cylinder.

spanwise three dimensionality, but, in fact, are associated with pronounced concentrations of small-scale streamwise vorticity.

4. DUAL VIEW SYSTEM FOR FLOW REGIONS WITH HIGH ASPECT RATIO

The overall goal of this type of quantitative imaging is to provide instantaneous views of the flow structure over, for example, the entire spanwise extent of a cylinder having a relatively large length-to-diameter ratio. It is, of course, desired to maintain adequate spatial resolution, in order to characterize the evolution of patterns of instantaneous velocity and vorticity in the near-wake. A representative configuration is a long vertical cylinder in a wave tank. The present aim is to characterize the variations of the direction of transverse vortex shedding along the span of the cylinder. Such a variation is an indicator of the spanwise coherence of vortex shedding, and thereby the transverse force on the cylinder. It is well known that time-dependent variations of the transverse force on a vertical cylinder in a wave can exhibit substantial modulations. The issue is to what degree such modulations can be associated with spontaneous transformation between states of three-dimensionality.

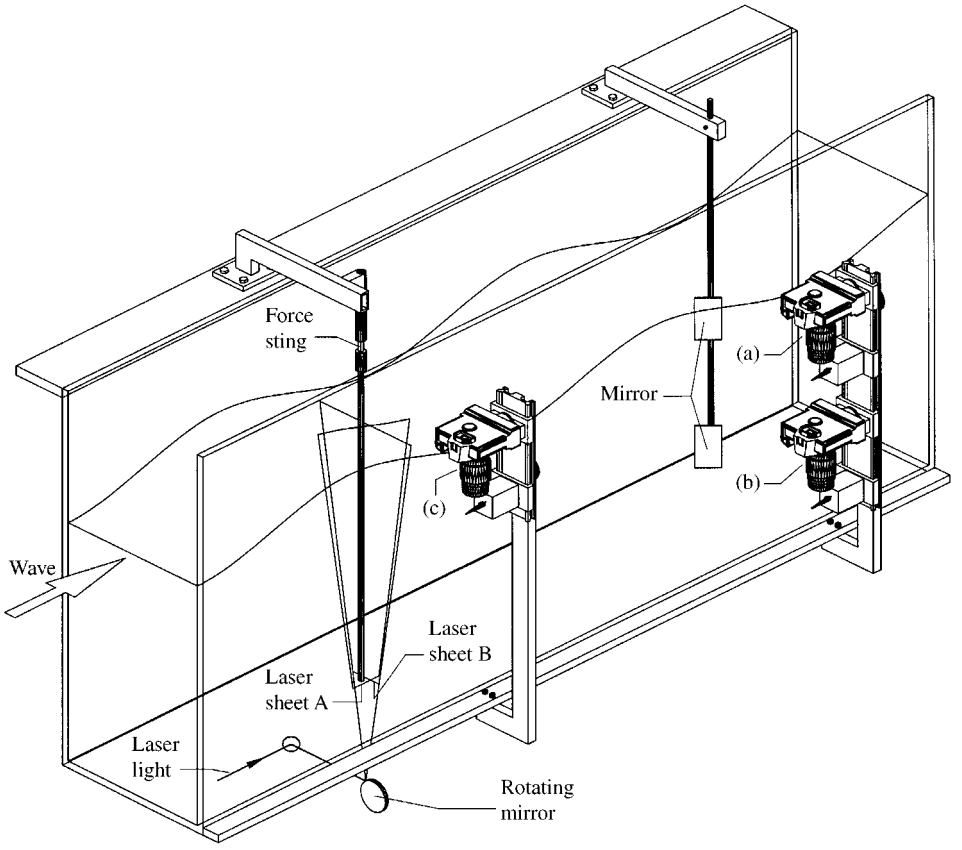

Figure 3. Schematic of experimental system illustrating wave tank, laser sheets, and orientations and arrangements of cameras employed for high-image-density particle image velocimetry.

For the particular case of a cylinder subjected to unidirectional oscillations in quiescent fluid or, conversely, a stationary cylinder in a flow undergoing unidirectional oscillations, Honji (1981), Sarpkaya (1986), and Tatsumo & Bearman (1990) have effectively characterized the patterns of spanwise-periodic three dimensionality using qualitative visualization. These studies vividly show that the spanwise wavelength of these patterns can range from approximately one cylinder diameter to several cylinder diameters. Furthermore, in the experiments of Obasaju *et al.* (1988), particle visualization taken simultaneously at two cross-sections along the span of the cylinder clearly suggests the existence of three dimensionality. With regard to numerical simulations of such three-dimensionality, the recent investigation of Duetsch *et al.* (1998) shows well-defined, spanwise periodic structure along the cylinder. The present emphasis is on the case of an actual free surface wave incident upon a vertical cylinder. The orbital particle trajectories of the wave, along with the different boundary conditions at the free surface and bottom (solid) surface of the wave tank are expected to significantly alter the nature of the three-dimensionality. Characterization of the spanwise structure of the near-wake, either for the aforementioned case of unidirectional flow or cylinder motion, or orbital motion of an actual wave, has not yet been pursued using high-image-density particle image velocimetry.

An overview of the imaging system, in conjunction with the wave tank, is given in Figure 3. Of principal interest for our present considerations is the PIV imaging technique.

Complete details of this approach, as well as descriptions of corresponding shadowgraph and force measurement techniques, are given by Yang, Lin & Rockwell (2000). The wave tank was custom-designed in order to allow optical access on all three sides. It is constructed of high-quality one-half inch glass suspended in a metal frame. As indicated in Figure 3, cameras (a) and (b) are employed for the dual end view, and camera (c) for a side view. Emphasis herein is on laser sheet orientation B, which is orthogonal to the direction of wave propagation. The location and orientation of the multi-faceted rotating mirror (48 facets) that generates this laser sheet is indicated beneath the wave tank. The plane of laser sheet B is located at a distance of 5 mm from the surface of the cylinder, which has a diameter of $D = 12{\cdot}7$ mm. Two small mirrors were located a distance of 1190 mm away from the centerline of the cylinder. Each of these mirrors had dimensions of 64 mm $\times$ 114 mm; they reflected the images from the upper and lower regions of the cylinder to the bias mirrors of each of the mirror–camera systems (a) and (b). The total distance from the plane of the laser sheet B to the image steering mirror within the wave tank, then to the bias mirror, and through the lens of the camera to the camera back was 1580 mm. For each of the cameras (a) and (b), the value of magnification was $M = 1:11$. The field of view in the plane of the laser sheet was 264 mm $\times$ 396 mm. Considering both of the adjacent images together, a total of approximately 12 000 velocity vectors were obtained. Both cameras (a) and (b), and their respective bias mirrors, were synchronized using a laboratory microcomputer. The fields of view of the images acquired by cameras (a) and (a) were adjusted such that they overlapped by $2D$ in the plane of the laser sheet. This approach allowed acquisition of two instantaneous images covering the entire span of the cylinder of submerged length $L = 700$ mm and aspect ratio $L/D = 55$.

A representative pattern of instantaneous velocity vectors in the crossflow plane is illustrated in the left image of Figure 4. It is evident that, at this instant, the velocity vectors have a substantial vertical component in the region beneath the free surface due to the orbital-like motion of the incident wave. Of particular interest herein is the manner in which the transverse (horizontal) velocity component varies along the span of the cylinder. As confirmed by independent vorticity measurements, the direction of the local transverse velocity corresponds to the direction of the vortex formation in the wake of the cylinder. When a given pattern of vortices forms, it sweeps fluid in a preferred direction from the base of the cylinder. Contours of constant transverse (horizontal) velocity are indicated in the right image of Figure 4. It is evident that these contours take on a quasi-periodic variation along the span of the cylinder. They have a longer wavelength between successive zero crossings at locations immediately beneath the free surface, where the orbital trajectory of the incident wave has a significant vertical component. On the other hand, this distance between zero crossings is relatively small near the bottom of the cylinder, where the incident wave is essentially unidirectional. Other admissible patterns of the near-wake, as well as aspects related to the measurement of the instantaneous transverse and in-line forces, are described by Yang & Rockwell (2000).

5. DUAL VIEW SYSTEM FOR FLOWS CONTAINING LONG BODIES ALONG THE AXIS OF VIEW

A cylinder in a wave gives rise to patterns of vortex formation that exist over the entire region about the periphery of the cylinder. That is, the vorticity concentrations are not swept away from the cylinder by a steady current. A single camera cannot adequately capture the features of the flow field surrounding the cylinder when the distance from the end of the cylinder to the cross-section of interest is relatively large, especially for the case where elastic oscillations occur. This situation arises for the case of a long vertical cylinder

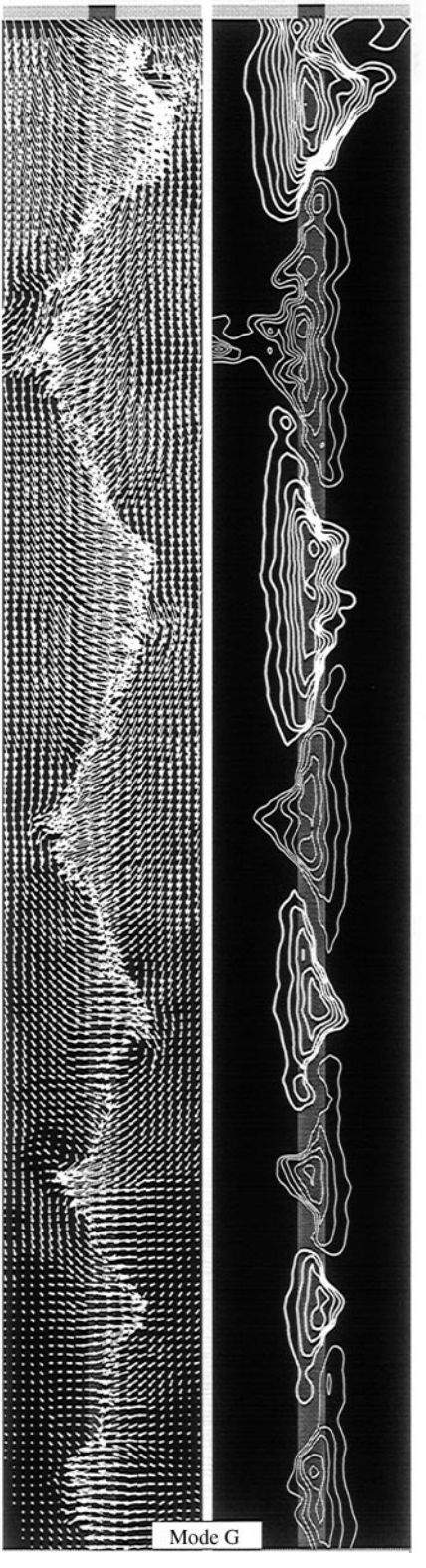

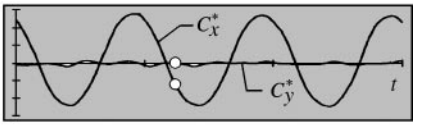

Figure 4. Patterns of instantaneous velocity determined from PIV measurements in laser sheet B in Figure 3. The left image shows patterns of velocity vectors, while the right image exhibits contours of constant horizontal velocity. Thick and thin white lines represent, respectively, positive (rightward) and negative (leftward) horizontal velocity. These patterns of velocity indicate the local direction of transverse vortex shedding in the near-wake of the cylinder. Value of Keulegan–Carpenter number is KC = 10.

in a wave tank. Quantitative imaging in a horizontal plane immediately beneath the free-surface must be accomplished through the bottom of the wave tank, due to refraction effects associated with the undulating free surface.

Major issues are the manner of generation of vorticity concentrations from the oscillating cylinder and the rate of decay of quasi-two-dimensional concentrations in the wave field. The physics of vortex formation from an oscillating, cantilevered vertical cylinder in a wave has been characterized by Borthwick & Herbert (1988) and Kaye (1989). They employed qualitative visualization to observe patterns of vortex formation at the free surface. Interpretation of this type of vortex formation, based on quantitative imaging, has yet to be undertaken. In doing so, it is necessary to account for the instantaneous relative velocity of the wave with respect to the cylinder when making an assessment of the instantaneous patterns of vorticity, which, in turn, are intimately related to not only the cylinder trajectory, but also to the forces on the cylinder.

Figure 5 shows side and plan views of the elastically mounted cylinder system. In essence, the vertical cylinder was attached to a lightweight hover plate, which remained suspended above a system of approximately 300 mini-jets that emanated from the top surface of a circular air plenum in the form of a donut. Four springs were employed to provide the desired stiffness. The system stiffness is essentially invariant in the circumferential direction. The cylinder is made of hollow Plexiglas in order to minimize its mass. At one section of the cylinder, a nonrefractive window, similar to that in Figure 1, is employed to allow illumination about the entire periphery of the cylinder. A horizontal laser sheet was generated immediately beneath the free surface of the wave by employing a long rectangular beam steering mirror. This mirror had dimensions of 610 mm $\times$ 102 mm. The scanning laser beam from the multi-faceted polygon mirror was reflected from this first-surface mirror at an angle of 90°, thereby forming the horizontal, scanning laser sheet. The scanning rate was 180 c/s. Two camera-bias mirror systems were employed for image acquisition, as indicated in Figure 5. The centerlines of the lenses of the two-camera system were displaced from each other by a distance of 140 mm. This spacing was found to be optimal for viewing the complete field about the periphery of the cylinder. The distance from the plane of the laser sheet to the back of each camera was 1180 mm. Both camera-bias mirror systems were synchronized using the laboratory microcomputer. Taking the images of the two cameras together, the field of view was 262 mm $\times$ 314 mm in the physical plane of the laser sheet. A total of 1650 velocity vectors were typically acquired in each camera view, giving a total of approximately 3000 vectors, excluding duplicate vectors in the region of image overlap.

Figure 6 shows a representative pattern of vorticity concentrations, along with the trajectory of the cylinder, which has the form resembling the outline of a "butterfly" pattern. The instant of image acquisition corresponds to the solid symbol 1 on the trajectory. At this instant, the cylinder is undergoing the initial phase of its transverse motion across the wave tank. The symbol U represents the instantaneous wave velocity, V_c is the cylinder velocity, and V_R is the relative velocity of the wave with respect to the cylinder. Vorticity concentrations C and A were shed during previous portions of the trajectory and concentrations B are in the process of formation from the surface of the cylinder. A full description of the admissible patterns of vortex formation, in relation to the instantaneous values of V_R, is given by Downes & Rockwell (2000).

6. CONCLUDING REMARKS

The approaches of high-image-density particle image velocimetry described herein hopefully will serve as a stimulus for further efforts, not only for the wake of a circular cylinder, but also for a broader range of flow systems that involve generation of unsteady separated

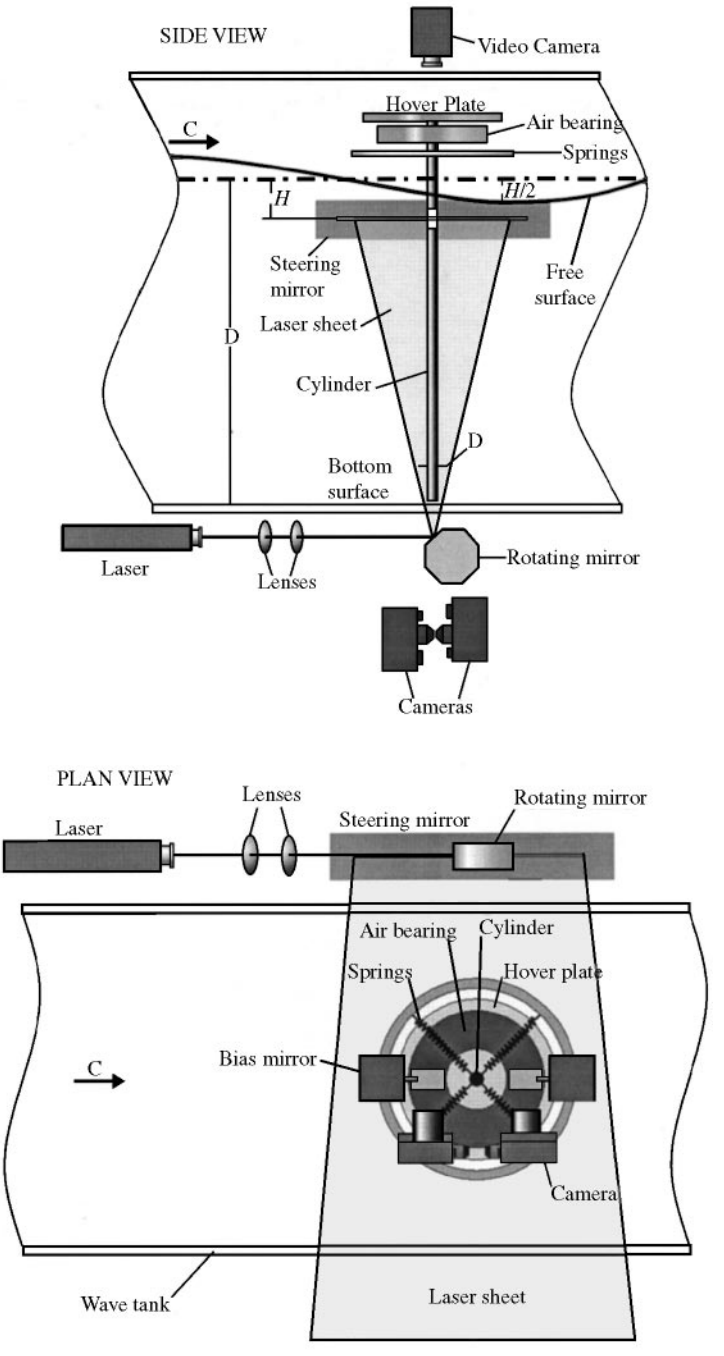

Figure 5. Schematics illustrating plan and side views of elastically mounted cylinder in conjunction with laser illumination for high-image-density particle image velocimetry. The plan view is upwards through the bottom of the wave tank.

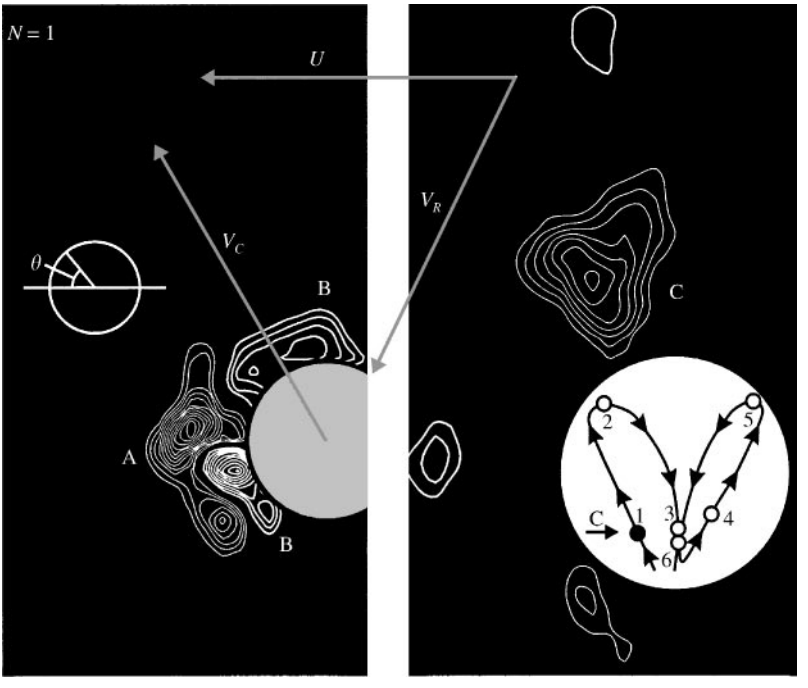

Figure 6. Patterns of positive (thick line) and negative (thin line) vorticity from a cylinder undergoing oscillations in a "butterfly" trajectory, as indicated in the inset. The location of the cylinder corresponds to point 1, which is designated by the black dot. Minimum vorticity level is $\omega_{\min} = 5\ s^{-1}$ and incremental vorticity is $\Delta\omega = 2{\cdot}5\ s^{-1}$. Velocity vectors correspond to: V_c = velocity of the cylinder; U = particle velocity of undisturbed region of wave adjacent to cylinder; and V_R = relative particle velocity of wave with respect to the cylinder.

flow in conjunction with unsteady loading, vibration, and noise. These methods are intended to serve as a complement to measurements of unsteady forces and surface pressures, though certain information on the surface loading can be estimated directly from this type of quantitative imaging, provided that the near-wake can be approximated as two-dimensional. Irrespective of the complexity of the wake structure, this type of imaging is also intended to provide guidance for development of corresponding numerical simulations.

The first two approaches, which involve imaging in orthogonal planes and in dual planes located adjacent to each other, aim to define the critical features of spanwise three-dimensionality, both for stationary and oscillating bodies. Although a full volume representation has not been addressed, acquisition of a space–time sequence of such images can lead to construction of a pseudo-volume representation, which can provide further insight into the three dimensionality of the wake. Furthermore, both of these approaches directly yield patterns of instantaneous velocity and vorticity over a defined plane. Using a sequence of images, it is possible to calculate, for example, the spanwise spatial correlation or the cross-spectral density in a direction parallel to the axis of the cylinder. Such calculations could be coupled with classical, time-averaged spanwise correlations of surface pressure, as well as measurement of forces. This type of comparison can provide insight into the physics related to traditional measurements of surface loading.

The third approach described herein involves imaging in dual planes, with emphasis on the quasi-two-dimensional features of the cylinder wake. It involves synchronized

acquisition of two images, which cover the entire periphery of an oscillating body, and aims to overcome the occurrence of blind regions or shadows due to blockage of the cylinder. This issue is particularly important for oscillatory flows past a stationary body, or conversely an oscillating body in quiescent fluid, both in absence of a steady current. Knowledge of the patterns of vorticity in the entire domain about the body, as a function of time, can provide insight into the rate of decay of peak vorticity and circulation of individual vorticity concentrations in either a unidirectional oscillatory flow or an inherently three-dimensional wave field.

All of the foregoing approaches are under continuous development. Part of this effort involves their implementation for digital camera systems. Rapid advances in both spatial and temporal resolution of image acquisition systems are expected in coming years.

ACKNOWLEDGEMENTS

Primary support for this research program was provided by the Office of Naval Research Grant No. N00014-94-1-0185, P00007, monitored by Dr Thomas Swean. In addition, supplemental support was provided by the Office of Naval Research Grant Nos. N00014-98-1-0817 and N00014-99-1-0581, AFOSR Grant No. F49620-99-1-0011 and NSF Grant CTS-9803734. The authors gratefully acknowledge this financial support.

REFERENCES

ADRIAN, R. J. 1986 Image-shifting technique to resolve directional ambiguity in double-pulsed velocimetry. *Applied Optics* **25,** 3855–3858.

ADRIAN, R. J. 1991 Particle-imaging techniques for experimental fluid mechanics. *Annual Review of Fluid Mechanics* **23,** 361–304.

ADRIAN, R. J. 1995 Limiting resolution of particle image velocimetry for turbulent flow. In *Advances in Turbulence Research—1995* (ed. M. J. Lee), pp. 1–19. Pohang, Korea: Turbulence Research Association.

ADRIAN, R. J. & YAO, C.-S. 1984 Development of pulsed laser velocimetry (PLV) for measurement of turbulent flow. In *Proceedings of the Ninth Symposium on Turbulence* (eds X. Reed, G. Patterson & J. Zakin), pp. 170–186. Rolla, MO: University of Missouri.

ATSAVAPRANEE, P., BENAROYA, H. & WEI, T. 1998 Vortex dynamics in the near-wake of a freely-oscillating cylinder. In *Proceedings of the 1998 Conference on Bluff-Body Wakes and Vortex-Induced Vibration* (eds P. W. Bearman & C. H. K. Williamson), Paper No. 5. Ithaca, NY: Cornell University.

BEARMAN, P. W. & WILLIAMSON, C. H. K. (eds) 1998 *Advances in Understanding of Bluff Body Wakes.* "Forum" at the 1998 ASME Fluids Engineering Division Summer Meeting, Washington, DC, 21–25 June.

BEARMAN, P. W., LEWEKE, T. & WILLIAMSON, C. H. K. (eds) 2000 *IUTAM Symposium on Bluff Body Wakes and Vortex-Induced Vibrations* (*BBVIV*2), Book of Abstracts, 13–16 June, Marseille, France.

BORTHWICK, A. G. L. & HERBERT, D. M. 1988 Loading and response of a small diameter flexibly mounted cylinder in waves. *Journal of Fluids and Structures* **2,** 479–501.

BREDE, M., ECKELMANN, H. & ROCKWELL, D. 1996 On secondary vortices in the cylinder wake. *Physics of Fluids* **8,** 2117–2124.

CETINER, O. & ROCKWELL, D. 2000 Near-wake structure of an oscillating cylinder: Imaging in orthogonal planes (in preparation).

CHYU, C.-K. & ROCKWELL, D. 1996*a* Near-wake structure of an oscillating cylinder: effect of controlled shear-layer vortices. *Journal of Fluid Mechanics* **322,** 21–49.

CHYU, C.-K. & ROCKWELL, D. 1996*b* Evolution of patterns of streamwise vorticity in the turbulent near-wake of a circular cylinder. *Journal of Fluid Mechanics* **320,** 117–137.

DOWNES, K. & ROCKWELL, D. 2000 Oscillations of a vertical elastically-mounted cylinder in a wave: imaging of vortex patterns (in preparation).

DUETSCH, H., DURST, F., BECKER, S. & LIENHART, H. 1998 Low-Reynolds-number flow around an oscillating circular cylinder at low Keulegan–Carpenter numbers. *Journal of Fluid Mechanics* **360,** 249–271.

ECKELMANN, H., GRAHAM, J. M. R., HUERRE, P. & MONKEWITZ, P. A. (eds) 1992 *Bluff Body Wakes, Dynamics and Instabilities.* Berlin: Springer-Verlag.

GERRARD, J. H. 1978 The wakes of cylindrical bluff bodies at low Reynolds number. *Philosophical Transactions of the Royal Society* (*London*) A **288,** 351–382.

GU, W., CHYU, C. & ROCKWELL, D. 1994 Timing of vortex formation from an oscillating cylinder. *Physics of Fluids* **6,** 3677–3682.

GU, W. & ROCKWELL, D. 1995 Flow structure from an oscillating cylinder with a localized nonuniformity: patterns of coherent vorticity concentrations. *Physics of Fluids* **7,** 993–998.

HAMA, F. R. 1957 Three-dimensional vortex pattern behind a circular cylinder. *Journal of Aeronautical Science* **24,** 156–158.

HONJI, H. 1981 Streaked flow around an oscillating circular cylinder. *Journal of Fluid Mechanics* **107,** 509–520.

KAYE, D. 1989 Oscillation of a vertical cylinder in waves. Ph.D. dissertation, University of Cambridge, Cambridge, U.K.

KEANE, R. D. & ADRIAN, R. J. 1990 Optimization of particle image velocimeters. Part I: double pulsed systems. *Measurement Science and Technology* **1,** 1202–1215.

KEANE, R. D. & ADRIAN, R. J. 1991 Optimization of particle image velocimeters: Part II: multiple pulsed systems. *Measurement Science and Technology* **2,** 963–974.

LANG, A. W. & GHARIB, M. 1998 On the effects of surface contamination in the wake of surface-piercing cylinder. In *Proceedings of the* 1998 *Conference on Bluff-Body Wakes and Vortex-Induced Vibrations* (eds P. W. Bearman & C. H. K. Williamson), Paper No. 28. Ithaca, NY: Cornell University.

LEE, S. D., CHUNG, S. H. & KIHM, K. D. 1996 Suggestive correctional methods for PIV image biasing caused by a rotating mirror system. *Experiments in Fluids* **21,** 201–208.

LIGHTHILL, J. 1986 Fundamentals concerning wave loading on offshore structures. *Journal of Fluid Mechanics* **173,** 667–681.

LIN, J.-C. & ROCKWELL, D. 1994 Cinematographic system for high-image-density particle image velocimetry. *Experiments in Fluids* **17,** 110–118.

LIN, J.-C. & ROCKWELL, D. 1996 Force identification by vorticity fields: techniques based on flow imaging. *Journal of Fluids and Structures* **10,** 663–668.

LIN, J.-C. & ROCKWELL, D. 1997 Quantitative interpretation of vortices from a cylinder oscillating in quiescent fluid. *Experiments in Fluids* **23,** 99–104.

LIN, J.-C. & ROCKWELL, D. 1999 Cinema PIV and its application to impinging vortex systems. *ASME Journal of Fluids Engineering* **121,** 720–724.

LIN, J.-C., SHERIDAN, J. & ROCKWELL, D. 1996*a* Near-wake of a perturbed, horizontal cylinder at a free-surface. *Physics of Fluids* **8,** 2107–2116.

LIN, J.-C., TOWFIGHI, J. & ROCKWELL, D. 1995 Near-wake of a circular cylinder: control by steady and unsteady surface injection. *Journal of Fluids and Structures* **9,** 659–669.

LIN, J.-C., VOROBIEFF, P. & ROCKWELL, D. 1996*b* Space–time imaging of a turbulent near-wake by high-image-density particle image cinematography. *Physics of Fluids* **8,** 555–564.

LOURENCO, L. M. & WHIFFEN, M. C. 1986 Laser speckle methods in fluid dynamics applications. In *Laser Anemometry and Fluid Mechanics—II* (eds R. Adrian, D. Durão, F. Durst, H. Mishina & J. Whitelaw), pp. 51–68. Lisbon: Ladoan-Inst. Super. Tec.

NOCA, F. 1996 On the evaluation of instantaneous fluid-dynamic forces on a bluff body. GALCIT Report FM96-5, California Institute of Technology, Pasadena, CA, U.S.A.

NOCA, F. 1997 On the evaluation of time-dependent fluid dynamic forces on bluff bodies. Ph.D. dissertation, California Institute of Technology, Pasadena, CA, U.S.A.

NOCA, F., SHIELS, D. & JEON, D. 1997 Measuring instantaneous fluid dynamic forces on bodies using only velocity field and their derivatives. *Journal of Fluids and Structures* **11,** 345–350.

NOCA, F., PARK, H. G. & GHARIB, M. 1998 Vortex formation length of a circular cylinder ($300 < Re < 4{,}000$) using DPIV. In *Proceedings of the* 1998 *Conference on Bluff-Body Wakes and Vortex-Induced Vibration* (eds P. W. Bearman & C. H. K. Williamson), Paper No. 46. Ithaca, NY: Cornell University.

NOCA, F., SHIELS, D. & JEON, D. 1999 A comparison of methods for evaluating time-dependent fluid dynamic forces on bodies, using only velocity fields and their derivatives. *Journal of Fluids and Structures* **13,** 551–578.

OBASAJU, E. D., BEARMAN, P. W. & GRAHAM, J. M. R. 1988 A study of forces, circulation and vortex patterns around a circular cylinder in oscillating flow. *Journal of Fluid Mechanics* **196,** 467–494.

OSCHWALD, M., BECHLE, S. & WELKE, S. 1995 Systematic errors in PIV by realizing velocity offsets with the rotating mirror method. *Experiments in Fluids* **18,** 329–334.

RAFFEL, M. & KOMPENHANS, J. 1995 Theoretical and experimental aspects of image-shifting by means of a rotating mirror system for particle image velocimetry. *Measurement, Science and Technology* **6,** 795–808.

ROCKWELL, D. 1998 Quantitative imaging of flow–structure interactions. In *Thirteenth Australasian Fluid Mechanics Conference* (eds M. C. Thompson & K. Hourigan), pp. 707–711. Melbourne, Australia: Monash University.

ROCKWELL, D. 2001 Imaging of unsteady separated flows: global approaches to new insight. Special Issue of *Experiments in Fluids* (in press).

ROCKWELL, D., MAGNESS, C., TOWFIGHI, J., AKIN, O. & CORCORAN, T. 1993 High image-density particle image velocimetry using laser scanning techniques. *Experiments in Fluids* **14,** 181–192.

SARPKAYA, T. 1986 Force on a circular cylinder in viscous oscillatory flow at low Keulegan–Carpenter numbers. *Journal of Fluid Mechanics* **165,** 61–71.

SHERIDAN, J., LIN, J.-C. & ROCKWELL, D. 1997 Flow past a cylinder close to a free-surface. *Journal of Fluid Mechanics* **330,** 1–30.

SHERIDAN, J., CARBERRY, J., LIN, J.-C. & ROCKWELL, D. 1998 On the near-wake topology of an oscillating cylinder. *Journal of Fluids and Structures* **12,** 215–220.

SUMNER, D., PRICE, S. J. & PAÏDOUSSIS, M. P. 1998 Investigation of side-by-side circular cylinders in steady cross-flow, by particle image velocimetry. In *Proceedings of the Conference on Bluff-Body Wakes and Vortex-Induced Vibration* (eds P. W. Bearman & C. H. K. Williamson), Paper No. 37. Ithaca, NY: Cornell University.

SUMNER, D., PRICE, S. J. & PAÏDOUSSIS, M. P. 2000 Flow-pattern identification for two staggered circular cylinders in cross-flow. *Journal of Fluid Mechanics* **411,** 263–303.

TATSUMO, M. & BEARMAN, P. W. 1990 A visual study of the flow around an oscillating circular cylinder at low Keulegan–Carpenter numbers and low Stokes numbers. *Journal of Fluid Mechanics* **211,** 157–182.

TECHET, A. H. & TRIANTAFYLLOU, M. S. 1998 The evolution of a '*hybrid*' shedding mode. In *Proceedings of the* 1998 *Conference on Bluff-Body Wakes and Vortex-Induced Vibration* (eds P. W. Bearman & C. H. K. Williamson), Paper No. 4. Ithaca, NY: Cornell University.

TOWFIGHI, J. & ROCKWELL, D. 1994 Flow structure from an oscillating nonuniform cylinder: generation of patterned vorticity concentrations. *Physics of Fluids* **6,** 531–536.

UNAL, M. F., LIN, J.-C. & ROCKWELL, D. 1997 Force prediction by PIV imaging: a momentum-based approach. *Journal of Fluids and Structures* **11,** 965–971.

WILLIAMSON, C. H. K. 1988 The existence of two stages in the transition to three-dimensionality of a cylinder wake. *Physics of Fluids* **31,** 3165–3168.

WILLIAMSON, C. H. K. 1992 The natural and forced formation of spot-like dislocations in the transition of a wake. *Journal of Fluid Mechanics* **243,** 393–441.

WILLIAMSON, C. H. K. 1996*a* Three-dimensional wake transition. *Journal of Fluid Mechanics* **328,** 345–408.

WILLIAMSON, C. H. K. 1996*b* Vortex dynamics in the cylinder wake. *Annual Review of Fluid Mechanics* **28,** 477–539.

WILLIAMSON, C. H. K., HESS, P., PETER, M. & GOVARDHAN, R. 1998 Fluid loading and vortex dynamics for a body in elliptic orbits. In *Proceedings of the Conference on Bluff-Body Wakes and Vortex-Induced Vibration* (eds P. W. Bearman & C. H. K. Williamson), Manuscript No. 18. Ithaca, NY: Cornell University.

WU, J. C. 1981 Theory for aerodynamic force and moment in viscous flows. *AIAA Journal* **19,** 432–441.

WU, J., SHERIDAN, J., HOURIGAN, K., WELSH, M. C. & THOMPSON, M. 1994 Longitudinal vortex structures in a cylinder wake. *Physics of Fluids* **6,** 2883–2885.

WU, J., SHERIDAN, J., WELSH, M. C. & HOURIGAN, K. 1996 Three-dimensional vortex structures in a cylinder wake. *Journal of Fluid Mechanics* **312,** 201–222.

YANG, Y., & ROCKWELL, D. 2000 Vertical cylinder in a wave: patterns of spanwise vortex formation and loading. Submitted to *Journal of Fluid Mechanics.*

ZHU, Q., LIN, J.-C., UNAL, M. F. & ROCKWELL, D. 2000 Motion of a cylinder adjacent to a free-surface: flow patterns and loading. *Experiments in Fluids* **28,** 559–575.